

# Allure of Craquelure: A Variational-Generative Approach to Crack Detection in Paintings

Laura Paul<sup>1,2</sup>, Holger Rauhut<sup>1,2</sup>, Martin Burger<sup>3,4</sup>, Samira Kabri<sup>3</sup>, Tim Roith<sup>3</sup>

<sup>1</sup>Dept. of Mathematics, LMU Munich, Germany  
 {paul, rauhut}@math.lmu.de

<sup>2</sup>Munich Center for Machine Learning, Germany

<sup>3</sup>Helmholtz Imaging, Deutsches Elektronen-Synchrotron DESY, Germany  
 {martin.burger, samira.kabri, tim.roith}@desy.de

<sup>4</sup>Fachbereich Mathematik, University of Hamburg, Germany

## Abstract

Recent advances in imaging technologies, deep learning and numerical performance have enabled non-invasive detailed analysis of artworks, supporting their documentation and conservation. In particular, automated detection of craquelure in digitized paintings is crucial for assessing degradation and guiding restoration, yet remains challenging due to the possibly complex scenery and the visual similarity between cracks and crack-like artistic features such as brush strokes or hair. We propose a hybrid approach that models crack detection as an inverse problem, decomposing an observed image into a crack-free painting and a crack component. A deep generative model is employed as powerful prior for the underlying artwork, while crack structures are captured using a Mumford–Shah-type variational functional together with a crack prior. Joint optimization yields a pixel-level map of crack localizations in the painting.

## Introduction

Advancements in imaging technologies, such as high-resolution photography, combined with recent breakthroughs in deep learning, have opened new avenues for the investigation, documentation, and conservation of artworks. These methods enable detailed analysis of the painting’s internal and surface structure in a non-invasive way, without the need for physical intervention, preserving the artwork’s integrity while offering deep insight into its material composition and condition [18]. A broad overview of the application of computational and mathematical tools to art investigation is provided in [18], emphasizing the relevance and the various prospects of interdisciplinary projects. A particularly important application of mathematical and computational techniques lies in the automated detection of *craquelure* patterns in digitized paintings, since cracks are among the most common forms of degradation found in aged artworks and carry significant information about the painting, such as its age, environmental history, and structural stability. Craquelure appears as a pattern of fine cracks in the paint surface, which can appear either dark or bright depending on the underlying paint and lighting conditions, for a first impression see Figure 1a. Detecting and analyzing the cracks accurately is essential for conservators in planning and executing restoration measures. One huge difficulty though is to develop methods that can distinguish cracks from visually similar elements such as brush strokes, canvas structure or painted hair, that are part of the original artistic process and appearance. Crack detection in digitized artworks using classic mathematical image processing methods dates back to the 1990s. Early works used morphological filters like the top-hat transformation in order to display cracks [10]. Similar methods were investigated in [20] for biomedical imaging in order to display vessel-like structures. After that, many works suggested morphological filtering in a prepossessing step plus different machine learning based methods to do fine-tuning in a postprocessing step in order to filter out crack-like structures as brush strokes or hair that had been falsely identified as cracks beforehand [9, 19, 4, 17, 16, 15]. Additionally, crack detection has been extensively studied with respect to damage in roads, see for example [21] [12]. Nevertheless, images in this setting are far less complex than artworks, and various datasets with ground truth annotations are readily available for training and evaluation, which are lacking in the arts context. In the following, we propose a novel approach to crack detection in digitized paintings that formulates the task as an

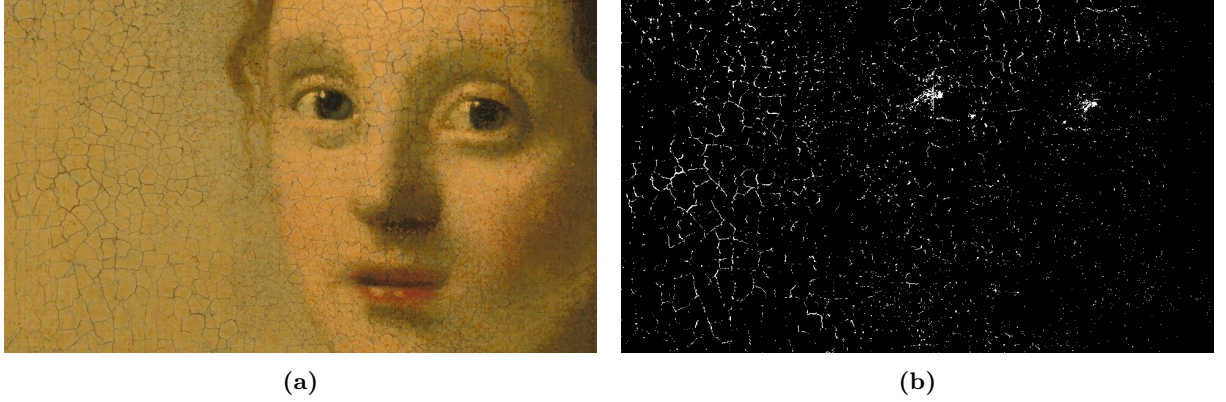


**Figure 1:** Qualitative example. (a) cropped detail from *The Lacemaker*, courtesy National Gallery of Art, and (b) predicted crack locations, where white pixels correspond to detected cracks.

inverse problem, combining a deep generative model with a Mumford–Shah-type functional to separate cracks from the underlying painting. Our method neither requires image preprocessing nor postprocessing beyond simple thresholding. It produces pixel-level binary maps localizing cracks in digitized artworks; Figure 1 offers a first appetizer of the results.

## Crack Detection in Digitized Paintings as Inverse Problem

In this work, the task of crack detection in images will be considered an *inverse problem*, thus we give a brief introduction on that topic based on [2] before formulating the problem in our precise setting. An inverse problem consists of recovering an unknown signal or parameter  $\mathbf{Y} \in \mathcal{Y}$  from measurements  $\mathbf{U} \in \mathcal{U}$  generated by a forward operator  $T : \mathcal{Y} \rightarrow \mathcal{U}$ , potentially corrupted by noise  $n$ , that is

$$\mathbf{U} = T(\mathbf{Y}) + n.$$

Inverse problems are said to be *ill-posed*, if the solution is sensitive to variations in data. More precisely, that is when at least one of the following fails: a solution may not exist for all measurements  $\mathbf{U}$  (existence), multiple  $\mathbf{Y}$  may explain the same  $\mathbf{U}$  (uniqueness), or small perturbations in  $\mathbf{U}$  may cause large deviations in  $\mathbf{Y}$  (stability). Such difficulties are very common, so regularization strategies are required to overcome them. In the context of crack detection,  $\mathbf{U} \in \mathcal{U} = \mathbb{R}^{h \times w \times 3}$  is the input RGB image, that is the digitized painting, and the goal is to recover the crack pattern  $\mathbf{L} \in \mathbb{R}^{h \times w}$  as well as the crack-free painting part  $\mathbf{B} \in \mathbb{R}^{h \times w \times 3}$  from it while the forward operator  $T$  maps  $(\mathbf{B}, \mathbf{L}) \in \mathcal{Y} = \mathbb{R}^{h \times w \times 4}$  to the observed image. Formally speaking, this can be expressed as a regularized inverse problem of the form

$$\min_{\mathbf{B}, \mathbf{L}} \underbrace{\mathcal{D}(T(\mathbf{B}, \mathbf{L}), \mathbf{U})}_{\text{data fidelity}} + \underbrace{\mathcal{R}_{\text{Painting}}(\mathbf{B}, \mathbf{L})}_{\text{painting prior}} + \underbrace{\mathcal{R}_{\text{Crack}}(\mathbf{L})}_{\text{crack prior}}.$$

- *Data fidelity*: The function  $\mathcal{D} : \mathcal{U} \times \mathcal{U} \rightarrow [0, \infty)$  compares the similarity of two measurements. Intuitively, the data fidelity measures, how likely it is that the measurement  $\mathbf{U}$  was created by the quantity  $(\mathbf{B}, \mathbf{L})$  and forward model  $T$ .
- *Painting prior*: The term *prior* originates from the Bayesian viewpoint, where before any measurement is taken we have a prior belief about the appearance of paintings  $\mathbf{B}$ . In the regularization formulation  $\mathcal{R}_{\text{Painting}}(\mathbf{B}, \mathbf{L})$  has small values for images  $\mathbf{B}$  with typical features and high values otherwise. The painting prior also receives the crack  $\mathbf{L}$  since it should not assess the painting in cracked regions.
- *Crack prior*: Similarly, the crack prior incorporates our prior belief on the shape of cracks  $\mathbf{L}$ .

In the following, we recall a classical mathematical framework for modeling images with discontinuities, namely the *Mumford–Shah functional*. For modeling purposes, in contrast to the previous discrete treatment, from now on we adopt a continuous formulation.

**Mumford–Shah formulation** The Mumford–Shah (MS) functional [13], originally introduced for image segmentation to approximate an image by a piecewise smooth function separated by a set of

discontinuities, provides a natural variational framework for modeling cracks, as the discontinuity set  $K$  corresponds to the crack locations from which the crack pattern  $\mathbf{L}$  is inferred. The MS regularizer is defined as

$$\mathcal{R}_{\text{MS}}(\mathbf{B}, K) = \int_{\Omega \setminus K} |\nabla \mathbf{B}|^2 dx + \mu \mathcal{H}^1(K),$$

where  $\Omega \subset \mathbb{R}^2$  is the image domain,  $\mathbf{B}$  is supposed to be in the Sobolev space  $H^1(\Omega \setminus K)$ ,  $K \subset \Omega$  denotes the set of discontinuities (edges),  $\mathcal{H}^1(K)$  its Hausdorff measure (length), and  $\mu > 0$  balances the edge length. This functional encourages  $\mathbf{B}$  to be smooth away from edges while allowing sharp discontinuities at crack locations. In practice, the MS functional is approximated using the *Ambrosio–Tortorelli* (AT) relaxation [1], introducing an auxiliary edge indicator function  $v : \Omega \rightarrow [0, 1]$ :

$$\mathcal{R}_{\text{AT}}(\mathbf{B}, v) = \underbrace{\int_{\Omega} v^2 |\nabla \mathbf{B}|^2 dx}_{\text{painting regularity}} + \mu \underbrace{\int_{\Omega} \left( \varepsilon |\nabla v|^2 + \frac{(v-1)^2}{4\varepsilon} \right) dx}_{\text{crack regularity}},$$

where  $\varepsilon > 0$  controls the smooth transition around cracks, and  $\mu$  weights the crack length. In this formulation,  $v \approx 0$  at crack locations and  $v \approx 1$  elsewhere, so it highlights cracks while allowing  $\mathbf{B}$  to be smooth between cracks. To highlight the distinction between the regularization performed on the painting and the one performed on the crack pattern, we denote the two terms separately by

$$\mathcal{R}_{\text{PReg}}(\mathbf{B}, v) := \int_{\Omega} v^2 |\nabla \mathbf{B}|^2 dx, \quad \mathcal{R}_{\text{CReg}}(v) := \int_{\Omega} \left( \varepsilon |\nabla v|^2 + \frac{(v-1)^2}{4\varepsilon} \right) dx.$$

Denoting by  $\odot$  pointwise multiplication, we then choose the data-fidelity term  $\mathcal{D}$  as

$$\mathcal{D}(T(\mathbf{B}, \mathbf{L}), \mathbf{U}) = \mathcal{D}(T(\mathbf{B}, v), \mathbf{U}) = \|v \odot (\mathbf{U} - \mathbf{B})\|_2^2,$$

so that the observed image is effectively compared to the background only in crack-free regions, since  $v$  is near zero at crack locations. To incorporate prior knowledge of plausible crack patterns, we employ a learned crack estimator  $P$ . This further helps to reduce false positives while preserving fine crack structures. More precisely, we introduce another regularization functional

$$\mathcal{R}_{\text{CP}}(\mathbf{U}', v) = \int_{\Omega} (v - P(\mathbf{U}'))^2 dx.$$

In this formulation  $P(\mathbf{U}') : \Omega \rightarrow [0, 1]$  gives an estimate of the crack pattern present in the input painting  $\mathbf{U}'$ , where values close to zero indicate cracks and values close to one correspond to crack-free regions. This encourages the predicted crack map to be consistent with the prediction obtained by  $P$ . We additionally optimize over the input  $\mathbf{U}'$  and initialize it with the original input image  $\mathbf{U}$ . We refer to the section on Numerical Experiments for details on the choice of  $P$ .

**Introducing a generative background prior** To further constrain the space of admissible crack-free paintings and to mitigate the ill-posedness of the decomposition, we model the background component  $\mathbf{B}$  using a deep generative prior. That is, we assume that  $\mathbf{B}$  lies in the range of a generator  $G : \mathcal{Z} \rightarrow \mathcal{X}$ , mapping from a low-dimensional latent space  $\mathcal{Z} \subset \mathbb{R}^d$  into the space of RGB images  $\mathcal{X}$ . Restricting  $\mathbf{B}$  to the generator range effectively constrains the solution to a learned manifold of plausible natural images, which has been shown to substantially reduce the ambiguity of ill-posed inverse problems [3, 6, 7]. In our setup, the latent variable  $z$  is optimized jointly with the crack indicator within the proposed variational formulation, allowing the generative prior to act as an implicit regularizer for the background reconstruction.

**The full optimization problem** Let  $G(z)$  denote the generative reconstruction of the crack-free painting and  $z$  its latent code. Combining the generative painting prior, the AT crack prior as well as the additional crack prior, we obtain the following full optimization problem

$$\min_{z, v, \mathbf{U}'} \|v \odot (\mathbf{U} - G(z))\|_2^2 + \lambda_{\text{PReg}} \mathcal{R}_{\text{PReg}}(G(z), v) + \lambda_{\text{CReg}} \mathcal{R}_{\text{CReg}}(v) + \lambda_{\text{CP}} \mathcal{R}_{\text{CP}}(P(\mathbf{U}'), v),$$

where the hyperparameters  $\lambda_{\text{PReg}}, \lambda_{\text{CReg}}, \lambda_{\text{CP}} > 0$  determine the influence of the different regularization terms. After optimization, the predicted pixel-level crack map is obtained as

$$\mathbf{L}_{\text{pred}} = 1 - v(x), \quad x \in \Omega,$$

so that brighter pixels correspond to probable crack locations.

## Numerical Experiments

In this section, we describe the implementation of the proposed approach and report crack detection results obtained on a synthetic dataset as well as on real-world cracked paintings. All experiments were performed on an NVIDIA A100 GPU. For both the representation of intact regions and the improved regularization of crack locations, we make use of existing machine learning models:

- For the generator  $G$  we use a fine-tuned version of the VQGAN model [8], pretrained on the ImageNet dataset [5]. VQGAN combines vector-quantized variational autoencoders with adversarial training, yielding a compact discrete latent representation that enables high-fidelity image synthesis while preserving local texture and structural consistency. This makes it well suited for modeling crack-free painting backgrounds, as it captures realistic material texture and spatial coherence without the blurring artifacts typical of pixel-space autoencoders.
- For the crack prior  $P$  we use a fine-tuned version of the DeepCrack model proposed in [12]. DeepCrack is a convolutional neural network that was trained on pavement images and outputs per-pixel crack probabilities from an input image.

**Datasets** A major challenge in crack detection for artworks is the lack of pixel-wise ground truth annotations. To quantitatively evaluate our approach and overcome this limitation, we construct a synthetic dataset of cracked paintings. As a basis, we use a self-curated dataset of approximately 8100 crack-free painting patches of size  $512 \times 512$  pixels. The source images are digitized paintings obtained from the National Gallery of Art (NGA), the Slovak National Gallery, and Wikimedia Commons. The synthetic dataset of approximately 1700 images with cracks is then generated by overlaying realistic crack patterns onto a subset of the crack-free painting patches. To obtain plausible crack geometries, we leverage publicly available pavement crack datasets, specifically CrackLS315 and CRKWH100 [12], using their binary ground-truth masks (see Figure 2b). The masks are blended into the painting images via an alpha-compositing model, where the crack appearance (dark or bright) is adaptively determined based on the average luminance of the underlying painting patch, as real craquelure can appear either bright or dark. The resulting images simulate realistic crack patterns with varying contrast and strength while preserving the original painting structure. Examples can be observed in Figure 2a.

**Fine-tuning of the machine learning models** In our experiments, the VQGAN model is not used in its original pretrained form. Instead, it is fine-tuned in an unsupervised manner on the self-curated dataset of around 8100 crack-free images. Fine-tuning is performed by unfreezing the last two encoder blocks, while keeping the codebook fixed and freezing the remaining encoder layers. The decoder and post-quantization convolution layers are trained to adapt the generator to the visual statistics of artworks. During fine-tuning, the generator is optimized using a combination of a pixel-wise reconstruction loss and a perceptual loss. The reconstruction loss is defined as an  $\ell_1$ -loss,

$$\mathcal{L}_{\text{rec}}(G(z), \mathcal{B}) = \|G(z) - \mathcal{B}\|_1,$$

which encourages accurate low-frequency and color reconstruction. In addition, a *perceptual loss* based on pretrained VGG features is employed,

$$\mathcal{L}_{\text{perc}}(G(z), \mathcal{B}) = \sum_l \|\phi_l(G(z)) - \phi_l(\mathcal{B})\|_2^2,$$

where  $\phi_l(\cdot)$  denotes the activation of the  $l$ -th layer. The total fine-tuning objective is then given by

$$\mathcal{L}_{\text{FT}} = \lambda_{\text{rec}} \mathcal{L}_{\text{rec}} + \lambda_{\text{perc}} \mathcal{L}_{\text{perc}}.$$

We set  $\lambda_{\text{rec}} = 0.65$  and  $\lambda_{\text{perc}} = 0.25$ , placing stronger emphasis on the  $\ell_1$  reconstruction loss to favor accurate pixel-level reconstruction of crack-free painting textures while the perceptual loss complements it to maintain semantic and structural consistency without over-smoothing fine details.

We further use a fine-tuned version of DeepCrack. The potential complex and diverse background of paintings, which may contain crack-like structures such as brush strokes or painted hair, poses a significant risk of false positive detections. Since the original DeepCrack model was trained on pavement datasets, we fine-tuned the model on a training subset of our synthetic dataset, in order to act as a good crack prior regardless the complex painting scene. More precisely, the side-outputs and fusion layer of the pretrained model were retrained in a supervised way, using a pixel-wise *Binary Cross-Entropy* (BCE)

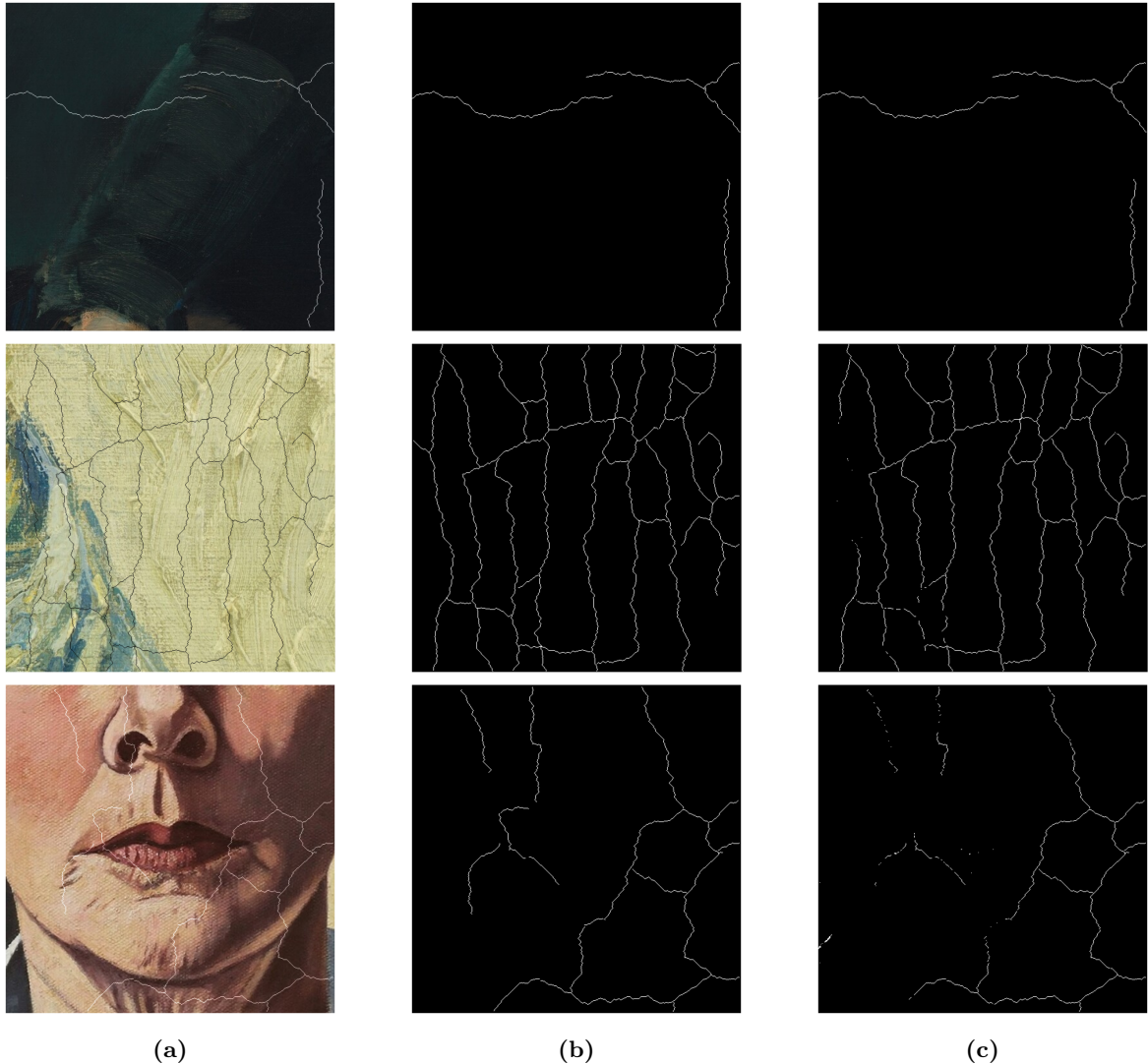


**Figure 2:** Qualitative results of the proposed VQGAN-AT crack detection framework on synthetic test data: (a) original input image, courtesy NGA and Wikimedia Commons, (b) ground-truth crack mask, and (c) predicted binary crack map obtained from the AT variable after Otsu thresholding.

loss. Given an input image  $\mathbf{U}'$  and the corresponding ground-truth crack mask  $M : \Omega \rightarrow \{0, 1\}$ , the BCE loss is defined as

$$\mathcal{L}_{\text{BCE}}(\mathbf{U}') = -\frac{1}{|\Omega|} \sum_{x \in \Omega} M(x) \log P(\mathbf{U}')(x) + (1 - M(x)) \log (1 - P(\mathbf{U}')(x)),$$

where  $P(\mathbf{U}')(x) \in [0, 1]$  refers to the predicted crack probability at pixel  $x \in \Omega$ .

**Solving the minimization problem** To minimize the variational functional, we perform gradient-based optimization over the painting latent representation  $z$ , the crack indicator  $v$ , and the crack prior input  $\mathbf{U}'$ . The resulting gradients are then used in an iterative scheme to update  $v$ ,  $z$  and  $\mathbf{U}'$  simultaneously until convergence. We employ the Adam optimizer [11] with separate learning rates for each variable. Further details on the optimization procedure are provided in the Appendix.

**Performance measure** We assess the crack detection performance by the *F1 score* (F1), which is a commonly used performance measure for binary classification tasks. It balances the trade-off between false positives and false negatives and is given by

$$\text{F1} = 2 \frac{\# \text{ crack pixels detected as crack pixels}}{\# \text{ pixels detected as crack pixels} + \# \text{ crack pixels}}.$$

**Regularization parameters and results** The outcome of the iterative reconstruction based on the variational functional heavily relies on its regularization parameters. We therefore perform a grid search over the parameters  $\lambda_{\text{PReg}}$ ,  $\lambda_{\text{CReg}}$ ,  $\lambda_{\text{CP}}$  as well as the weight  $\varepsilon$  that appears in the definition of  $\mathcal{R}_{\text{CReg}}$ . The parameter set achieving the highest F1 score on a held-out test subset of 200 synthetic image patches and masks is selected for all reported results. The resulting best parameters for our model are

$$\lambda_{\text{PReg}} = 1, \lambda_{\text{CReg}} = 0.1, \lambda_{\text{CP}} = 0.5 \text{ and } \varepsilon = 0.005.$$

The final crack map is computed from the optimized variable  $v$  as  $\mathbf{U}_{\text{pred}} = 1 - v$ , then a binary pixel-wise crack map is obtained by thresholding via Otsu's method [14]. Using the specified parameters, this yields a mean F1 score of 0.97 on the test dataset. In Figure 1 and 3 the performance of our approach on real world digitized painting can be observed. For such larger or high-resolution images files, crack maps are computed on overlapping patches using local thresholding. Soft crack maps are averaged in overlapping regions, while binary crack detections are merged using a logical OR to preserve thin structures. While the predicted crack maps clearly capture crack patterns, some non-crack structures, such as finger contours in Figure 3, are pushed into the background, whereas others, such as painted eye areas in the case of Figure 1, are falsely detected.



**Figure 3:** Qualitative crack detection result of the proposed VQGAN-AT framework on a real digitized painting with structural damage: (a) cropped detail from *The Mourning Madonna*, courtesy NGA, and (b) predicted binary crack map obtained from the AT variable after Otsu thresholding.

## Summary and Conclusions

In this work, we introduced a variational inverse problem formulation for crack detection in digitized paintings that combines classical image regularization with modern powerful learned priors. Crack detection is modeled as the joint recovery of a crack-free painting and a crack map, where the background

is represented by a pretrained and fine-tuned VQGAN model, while crack structures are recovered via a Mumford–Shah-type regularization guided by the output of the fine-tuned DeepCrack model. The proposed approach allows pixel-level crack localization without relying on image pre- or postprocessing, apart from a final thresholding step. Synthetic data generation using realistic crack patterns enables quantitative evaluation in the absence of annotated artwork datasets. The numerical experiments demonstrate that most crack structures are correctly identified while only few false positives are introduced, despite the presence of complex background textures. This indicates that crack detection in artworks can be effectively addressed as a regularized inverse problem with learned priors, offering an alternative to fully supervised approaches. Deep learning-guided variational models with generative image representations thus constitute a promising direction for crack detection and, more broadly, structural analysis in cultural heritage imaging. Nevertheless, subtle cracks may be missed, resulting in false negatives, while highly textured non-crack patterns and discontinuities in general can cause occasional false positives. One possible cause is that the synthetic dataset may not fully capture the diversity of natural aging patterns. Additionally, hyperparameters working best on the synthetic dataset may not be optimal for real-world images. Future work could investigate strategies to improve generalization. Furthermore, one could explore replacing the DeepCrack prior with an unsupervised crack prior in order to avoid reliance on annotated or synthetic datasets for training. This could, for example, involve a crack generator trained on unlabeled crack patterns.

## Appendix

Here, we provide more details on the reconstruction algorithm used within the paper. We intend to solve the following minimization problem

$$\min_{z, v, \mathbf{U}'} \underbrace{\|v \odot (\mathbf{U} - G(z))\|_2^2 + \lambda_{\text{PReg}} \mathcal{R}_{\text{PReg}}(G(z), v) + \lambda_{\text{CReg}} \mathcal{R}_{\text{CReg}}(v) + \lambda_{\text{CP}} \mathcal{R}_{\text{CP}}(P(\mathbf{U}'), v)}_{=:L(z, v, \mathbf{U}')}.$$

In practice we only work with discretized quantities, which means  $z \in \mathbb{R}^d$ ,  $\mathbf{U}, \mathbf{U}' \in \mathbb{R}^{h \times w \times 3}$ ,  $v \in [0, 1]^{h \times w}$ . In order to ensure that  $v$  only takes values in  $[0, 1]$ , we choose the following reparameterization

$$v := \sigma(s), \quad \sigma : \mathbb{R} \rightarrow \mathbb{R}, \quad \sigma(a) := \frac{e^a}{1 + e^a},$$

where  $\sigma$  is applied entry-wise to the elements of  $v$ . We then optimize over  $s$ , which ensures  $z \in [0, 1]^{h \times w}$ . As mentioned before, in order to compute an approximate solution to the above problem, we employ the Adam optimizer proposed in [11], which we repeat below in Algorithm 1, for the readers convenience.

---

**Algorithm 1** Adam optimizer adapted from [11]

**Input:** Diagonal step size matrix  $\Gamma = \text{diag}(\gamma_1, \dots, \gamma_p)$ , decay rates  $\beta_1, \beta_2 \in [0, 1)$ , objective function  $L : \mathbb{R}^p \rightarrow \mathbb{R}$ ,  $X_0 \in \mathbb{R}^p$  initial iterate, zero division margin  $\epsilon$

- 1:  $m_0 := 0 \in \mathbb{R}^p$
- 2:  $v_0 := 0 \in \mathbb{R}^p$
- 3: **for**  $k = 1 \dots, K$  **do**
- 4:    $g_k := \nabla L(X_{k-1})$
- 5:    $m_k := \beta_1 m_{k-1} + (1 - \beta_1) g_k$
- 6:    $v_k := \beta_2 v_{k-1} + (1 - \beta_2) (g_k \odot g_k)$
- 7:    $\hat{m}_k := m_k / (1 - (\beta_1)^k)$
- 8:    $\hat{v}_k := v_k / (1 - (\beta_2)^k)$
- 9:    $X_k := X_{k-1} - \Gamma (\hat{m}_k / (\hat{v}_k + \epsilon))$

**Return:**  $X_K$

---

For our reconstruction we use the standard decay rates  $\beta_1 = 0.9$ ,  $\beta_2 = 0.999$  and margin  $\epsilon = 10^{-8}$  as proposed in [11]. As the loss function, we choose  $(z, s, \mathbf{U}') \mapsto L(z, \sigma(s), \mathbf{U}')$  and set the step sizes as

$$\Gamma = \text{diag}(\underbrace{\gamma^z, \dots, \gamma^z}_{d \text{ times}}, \underbrace{\gamma^s, \dots, \gamma^s}_{h \cdot w \text{ times}}, \underbrace{\gamma^{\mathbf{U}'}, \dots, \gamma^{\mathbf{U}'}}_{h \cdot w \cdot 3 \text{ times}}),$$

with

$$\gamma^z = 0.005, \quad \gamma^s = 0.1, \quad \gamma^{\text{v}'} = 0.01.$$

## References

- [1] L. Ambrosio and V. M. Tortorelli. “Approximation of functional depending on jumps by elliptic functional via  $\Gamma$ -convergence.” *Communications on Pure and Applied Mathematics*, vol. 43, no. 8, 1990, pp. 999–1036.
- [2] S. Arridge, P. Maass, O. Öktem, and C.-B. Schönlieb. “Solving inverse problems using data-driven models.” *Acta Numerica*, vol. 28, 2019, pp. 1–174.
- [3] A. Bora, A. Jalal, E. Price, and A. G. Dimakis. “Compressed sensing using generative models.” *International conference on machine learning*. PMLR, 2017. pp. 537–546.
- [4] B. Cornelis, T. Ružić, E. Gezels, A. Dooms, A. Pižurica, L. Platiša, J. Cornelis, M. Martens, M. De Mey, and I. Daubechies. “Crack detection and inpainting for virtual restoration of paintings: The case of the Ghent Altarpiece.” *Signal Processing*, vol. 93, no. 3, 2013, pp. 605–619.
- [5] J. Deng, W. Dong, R. Socher, L.-J. Li, K. Li, and L. Fei-Fei. “Imagenet: A large-scale hierarchical image database.” *2009 IEEE conference on computer vision and pattern recognition*. IEEE, 2009. pp. 248–255.
- [6] A. G. Dimakis. *Deep Generative Models and Inverse Problems*. Cambridge University Press, 2022. p. 400–421.
- [7] M. Duff, N. D. Campbell, and M. J. Ehrhardt. “Regularising inverse problems with generative machine learning models.” *Journal of Mathematical Imaging and Vision*, vol. 66, no. 1, 2024, pp. 37–56.
- [8] P. Esser, R. Rombach, and B. Ommer. “Taming transformers for high-resolution image synthesis.” *Proceedings of the IEEE/CVF conference on computer vision and pattern recognition*. 2021. pp. 12873–12883.
- [9] I. Giakoumis, N. Nikolaidis, and I. Pitas. “Digital image processing techniques for the detection and removal of cracks in digitized paintings.” *IEEE Transactions on Image Processing*, vol. 15, no. 1, 2005, pp. 178–188.
- [10] I. Giakoumis and I. Pitas. “Digital restoration of painting cracks.” *ISCAS’98. Proceedings of the 1998 IEEE International Symposium on Circuits and Systems (Cat. No. 98CH36187)*. vol. 4. IEEE, 1998. pp. 269–272.
- [11] D. P. Kingma and J. Ba. “Adam: A method for stochastic optimization.” *3rd International Conference on Learning Representations, ICLR 2015*. 2015.
- [12] Y. Liu, J. Yao, X. Lu, R. Xie, and L. Li. “DeepCrack: A deep hierarchical feature learning architecture for crack segmentation.” *Neurocomputing*, vol. 338, 2019, pp. 139–153.
- [13] D. Mumford and J. Shah. “Optimal approximations by piecewise smooth functions and associated variational problems.” 1989.
- [14] N. Otsu *et al.* “A threshold selection method from gray-level histograms.” *Automatica*, vol. 11, no. 285–296, 1975, pp. 23–27.
- [15] C. Rucoba-Calderón, E. Ramos, and J. Gutiérrez-Cárdenas. “Crack detection in oil paintings using morphological filters and K-SVD algorithm.” *Annual International Conference on Information Management and Big Data*. Springer, 2021. pp. 329–339.
- [16] R. Sizyakin, B. Cornelis, L. Meeus, H. Dubois, M. Martens, V. Voronin *et al.* “Crack detection in paintings using convolutional neural networks.” *IEEE Access*, vol. 8, 2020, pp. 74535–74552.

- [17] R. Sizyakin, B. Cornelis, L. Meeus, M. Martens, V. Voronin, and A. Pizurica. “A deep learning approach to crack detection in panel paintings.” *Image Processing for Art Investigation (IP4AI)*. 2018. pp. 40–42.
- [18] B. Sober, S. Bucklow, N. Daly, I. Daubechies, P. L. Dragotti, C. Higgitt, J.-J. Huang, A. Pižurica, W. Pu, S. Reynolds *et al.* “Revealing and reconstructing hidden or lost features in art investigation.” *IEEE BITS the Information Theory Magazine*, vol. 2, no. 1, 2022, pp. 4–19.
- [19] G. S. Spagnolo and F. Somma. “Virtual restoration of cracks in digitized image of paintings.” *Journal of Physics: Conference Series*. vol. 249. no. 1. IOP Publishing, 2010. p. 012059.
- [20] F. Zana and J.-C. Klein. “Segmentation of vessel-like patterns using mathematical morphology and curvature evaluation.” *IEEE Transactions on Image Processing*, vol. 10, no. 7, 2001, pp. 1010–1019.
- [21] L. Zhang, F. Yang, Y. D. Zhang, and Y. J. Zhu. “Road crack detection using deep convolutional neural network.” *2016 IEEE International Conference on Image Processing (ICIP)*. IEEE, 2016. pp. 3708–3712.